Article

Two-Way Power Flow Balancing in Three-Phase Three-Wire Networks by Unbalanced Capacitive Shunt Compensation

Adrian Pană, Alexandru Băloi *, Florin Molnar-Matei , Cristian Stănese, Andrei Jorza and David Stoica

Power Engineering Department, Politehnica University Timisoara, V Parvan 2, 300223 Timisoara, Romania; adrian.pana@upt.ro (A.P.); florin.molnar@upt.ro (F.M.-M.); cristian.stanese@student.upt.ro (C.S.); andrei.jorza@student.upt.ro (A.J.); david.stoica@student.upt.ro (D.S.)
* Correspondence: alexandru.baloi@upt.ro; Tel.: +40-256-403-428

Abstract: Developed to achieve the balancing of three-phase loads and improve their power factor, the BCC (Balancing Capacitive Compensator) is presented in this paper as having a broader capability, namely that of balancing the two-way power flow. BCCs are becoming useful in today's distribution networks with a high content of DERs (Distributed Energy Resources), where unbalanced power transfers to the higher voltage network occur more and more frequently as a result of the excess power generated. The article contains a case study in which, by means of Matlab-Simulink 2021 modelling, such a network is studied by considering two regimes corresponding to the two-way power flow. The numerical analysis of phase components and sequence components confirms the validity of the mathematical model concerning the BCC and also for the case of changing the way of power flow in the section controlled by the compensator. This demonstrates the possibility of extending the load balancing function of the BCC to that of balancing the two-way power flow and is an additional argument in support of replacing, in the more or less near future, conventional shunt capacitive compensators with capacitive balancing compensators.

Keywords: distribution network; distributed energy resources; voltage unbalances; load balancing; unbalanced two-way power transfer; shunt capacitive compensation; balancing capacitive compensator; Matlab-Simulink model

1. Introduction

The accelerated growth in recent years of the number of single-phase and three-phase Distributed Energy renewable Resources (DERs), has caused a series of additional technical and economic problems, resulting from the need to ensure a high level of performance of the Electric Power Distribution Systems (EPDS) of low and medium voltage. Among these, the most important are:

- increasing the power transfer capacity of some lines (sections of lines), transformer substations or transformer stations;
- ensuring the technical conditions that allow for maximizing the energy generated by the distributed sources;
- ensuring the appropriate quality of power delivered to consumers by limiting the level of disturbances produced and propagated in the network (power frequency disturbances, electromagnetic interferences, transients, harmonics and low power factor, overvoltages, voltage fluctuations, voltage unbalances, etc. [1]).

The article refers to a particular disturbance present in the three-phase three-wire medium voltage distribution networks containing distributed sources of electrical energy: the active and reactive power flow unbalance on the three phases of lines and transformers, going in two ways through various sections of the network.

Unbalances in the active and reactive power flow in a medium voltage distribution network are determined by unbalanced loads fed directly from this network or resulting in

propagation from low-voltage networks. Over these the unbalances of active and reactive powers generated by single-phase wind or photovoltaic sources are superimposed, which are unevenly distributed, have an intermittent, variable, and non-simultaneous operation and are present, especially at the single-phase prosumers from the low-voltage networks connected to it. The phenomenon is amplified by the presence of an increasing number of electrical energy storage systems, an important part of which is represented by EVs (electric vehicles) that can be used as controllable loads, energy storage systems, or power supply sources [2].

An important characteristic of these networks is the fact that the operating regimes of DERs can hardly be correlated with those of consumers, thus resulting in numerous time intervals, longer or shorter, in which the generated power is in excess. In these time intervals, the excess power generated is transferred to the higher voltage network, which means changing the direction of power flow through the HV/MV transformer station. As a result of the accentuation of the unbalances, this change of direction is performed in one, two or three phases, at different times and for different durations. In fact, there is an increase in the propagation of unbalance disturbances in the higher voltage network.

The increase in power flow unbalances in the network is accompanied by the voltage asymmetry accentuation, the increase in the deviations of the rms voltage values above the admissible limits, the overloading of some sections of the current paths, and the pronounced decrease in the power factor [3]. These disturbances negatively affect the operation of distribution operators' installations by increasing the difficulties of operating the network, mainly in terms of voltage regulation systems, protection, and control systems, especially because of two-way power transfer.

The accentuation of voltage asymmetry in the points of common coupling (PCC—Point of Common Coupling) between the network and consumers can be considered as an accentuation of the quality deterioration of the energy delivered to consumers. The three-phase receivers, especially transformers and induction motors, are the most affected by this disturbance. In the case of the three-phase transformer, the asymmetry of the supply voltages causes the increase in losses in the copper and therefore the increase in the temperature in some areas inside. This results in a decrease in efficiency and a reduction in the lifetime of the transformer as a result of accelerating the ageing of the insulation [4,5]. As for the three-phase induction motor, the phenomena are similar and in addition, as a result of the mechanical torque oscillations and vibrations occurrence, there is an increase in mechanical wear [6,7].

The voltage balancing of the three-phase low and medium voltage networks containing DERs has become very important, both for the distribution network and the consumers connected to it and from the perspective of the propagation of disturbances in the higher voltage network. In the current specialized literature, there are studies related to a multitude of solutions consisting of new methods and equipment, or the improvement of the known ones. According to [8], the strategies for compensating voltage asymmetries in distribution networks containing DERs can be classified into two broad categories: active strategies and passive strategies.

Active strategies use active equipment, based on power electronics technology, with the main or secondary function of voltage asymmetry compensation. This category of equipment, known under the generic name of Switching Power Converters (SPCs), includes: Line Voltage Regulator (LVR) [9], advanced On-Load Tap Changer (OLTC) [10], Reactive Power Compensator (RPC) [11], Zero Sequence Current Compensator (ZSCC) [12], Distribution Static Synchronous Compensator (D-STATCOM) [13], Dynamic Voltage Restorer (DVR) [14], and Unified Power Quality Conditioner (UPQC) [15]. Although this equipment has very good technical performance, it is difficult to implement on a large scale, especially at high nominal unit powers, due to the costs, which are still very high.

A distinct category of active strategies is those based on the inverters in the composition of three-phase or single-phase DERs. In the case of three-phase DERs, the inverters can be controlled in such a way as to allow not only different values of active power injection

per phase but also the injection or absorption of reactive power of different values per phase, without disturbing the total amount of active power produced by the DER [16]. This control can also be performed in the case of single-phase DERs, but the balancing of power flow on phases requires the coordination of single-phase DERs installed on different phases [17]. The disadvantage of applying these strategies lies in the need for the DERs and the inverters in their composition to be of oversized nominal power to allow the application of the reactive power regulation function with the aim of symmetrizing the voltages on the network phases.

The same category of active strategies also includes DER-BESS (Battery Energy Storage System) combinations, the most famous of which is the Photo Voltaic (PV)–Electric Vehicle (EV) combination. They allow the charging or absorption of active powers per phase, so that, by optimizing the control algorithms of the charging and discharging regimes of the batteries, the optimization of the distribution network voltage symmetrization can be obtained [18].

Passive voltage symmetrization strategies, while not as efficient as active ones, are much less expensive and easier to implement on a large scale.

The first type of passive strategy is based on methods or techniques for reconfiguring feeders [19], changing load phases [20], optimizing the location of DERs [21], or combinations thereof [22].

Direct, single-phase voltage regulation can also be considered as a passive voltage symmetrization method. For this purpose, special transformers have been designed that allow voltage regulation, through the on-load switching of the taps, individually per phase [10].

One of the most important methods, which belongs to the category of passive strategies, is shunt-reactive compensation. The Balancing-Reactive power Compensator (BRC) originates from Steinmetz's assembly. It contains only passive reactive circuit elements, coils, or capacitor banks, which, in order to respond to the load variation, can be controlled or switched with power electronic devices [23,24], forming the so-called Adaptive Balancing Compensators (ABCs) [25], which are actually a particular form of SVC (Static Var Compensator). For the sizing and control of the component elements of the ABC, the method of symmetrical components [26] or the Current's Physical Components (CPC) concept [11] is usually used. In both cases, the ABC control is completed with the aim of compensating the unwanted components of the currents on the load phases.

Comparison based on technical–economic criteria between the two types of equipment designed for the power flow balancing on phases, SVC and SPC, respectively, is favourable to the first type, in the case of a series of applications, including that of distribution networks with a high level of DER penetration.

Thus, compared to SVCs, SPCs cause lower active energy losses and therefore have higher energy efficiency, since they contain few passive circuit elements. SPCs also have other clearly superior technical performances, including faster response times, and more compact structures so they demand less space, and generate lower noise. However, most of the SPCs need complicated calculations and high-frequency PWM techniques that reduce the main circuit efficiency, especially in high-power applications [27]. At the same time, in many industrial applications, the reaction speed or the precision of the compensation adjustment are not the main performance criteria, the decisive criterion being the cost of installing and operating the equipment. It is demonstrated that for applications with similar functions such as voltage regulation, power factor correction, load balancing or flicker diminishing, the acquisition and operating costs for an SVC are smaller by about 30–35% than for a SPC [28]. Therefore, not only the SVC type compensators are not being eliminated, but on the contrary, their use is developing, so the world market for such equipment is constantly growing [28].

BRCs (Balancing-Reactive Compensators) and BCCs (Balancing Capacitive Compensators) are also part of the SVC equipment category, known as three-phase load balancing means. These are the subject of the following sections of the article. Thus, the second

section is dedicated to the brief presentation of the mathematical relationships for sizing the primary circuits of a BRC (BCC), respectively, of those that allow the demonstration of the energy mechanism of balancing active and reactive inductive loads, by shunt unbalanced-reactive (capacitive) compensation. The fact that these relationships remain valid regardless of the direction of the active and reactive powers through the compensator-controlled section is demonstrated in section three, on a Simulink model of a medium voltage distribution network, for two-way unbalanced power flow operating conditions. This validates the possibility of extending the load balancing function, for which BCC is known until now, to that of balancing the two-way power flow through the sections of the distribution network.

The main contributions of the paper are:

- identification and analysis of unbalanced shunt capacitive compensation as a method of two-way power flow balancing in three-phase networks;
- demonstrating, based on the mathematical model, respectively, by numerical simulation, the ability of the BCC to extend its load balancing function as the two-way power flow balancing function in the controlled section;
- the conception and construction of the Simulink model, respectively, and the interpretation of the operating regimes numerical simulation results of a distribution network containing a high level of renewable distributed sources.

2. BCC—From Load Balancing to Power Flow Balancing

SVC-type equipment has found a very efficient application from a technical–economic point of view in three-phase network power flow balancing. According to a series of studies previously published by authors of this article, in a wide variety of situations, three-phase unbalanced loads can be perfectly balanced, simultaneously maximizing the power factor, by unbalanced shunt capacitive compensation [29–31], by using a BCC. Such a compensator offers, in addition to the advantage of a low cost, by eliminating the coils, the easy possibility to obtain a dynamic compensation, which follows the load variation, by automatically switching the steps of single-phase capacitor banks (ABCC—Adaptive Balancing Capacitive Compensator) [30,31].

In the case of three-phase three-wire networks, the compensator contains three batteries of single-phase capacitors in a delta connection (Figure 1). In addition to the usual functions of voltage regulation or power factor improvement, the compensator can perform the balancing of active and reactive powers consumed per phase. The mathematical model associated with the load-compensator assembly, expressed in phase components, shows that the energy balancing mechanism consists of the redistribution of active and reactive powers between the phases. By using positive–negative-zero sequence components, it is demonstrated that the compensator causes the negative sequence current flow, equal and sign opposite to the negative sequence currents of the load [23–25].

The following paragraphs briefly present the relationships for calculating the equivalent susceptances of the reactive elements of the respective compensator to illustrate the energy mechanism of load balancing, which will then allow the load balancing function to be extended to that of power flow balancing.

According to [26], the values of the three equivalent susceptances of the single-phase sides of the BCC can be calculated using the relationships derived based on a simplified mathematical model, in which it is considered that the three-phase assembly formed by the unbalanced equivalent load and the BCC, is connected to a source with a sufficiently large short-circuit power so that the asymmetries of the three-phase sets of the phase to ground voltages and the phase to phase voltages can be neglected. The unbalanced load, real or equivalent, can be modelled by a triangle of three equivalent admittances:

$$\begin{bmatrix} \underline{Y}_{ab}^{load} \\ \underline{Y}_{bc}^{load} \\ \underline{Y}_{ca}^{load} \end{bmatrix} = \begin{bmatrix} 1 & 0 & 0 \\ 0 & 1 & 0 \\ 0 & 0 & 1 \end{bmatrix} \cdot \begin{bmatrix} G_{ab}^{load} \\ G_{bc}^{load} \\ G_{ca}^{load} \end{bmatrix} - j \cdot \begin{bmatrix} 1 & 0 & 0 \\ 0 & 1 & 0 \\ 0 & 0 & 1 \end{bmatrix} \cdot \begin{bmatrix} B_{ab}^{load} \\ B_{bc}^{load} \\ B_{ca}^{load} \end{bmatrix} \qquad (1)$$
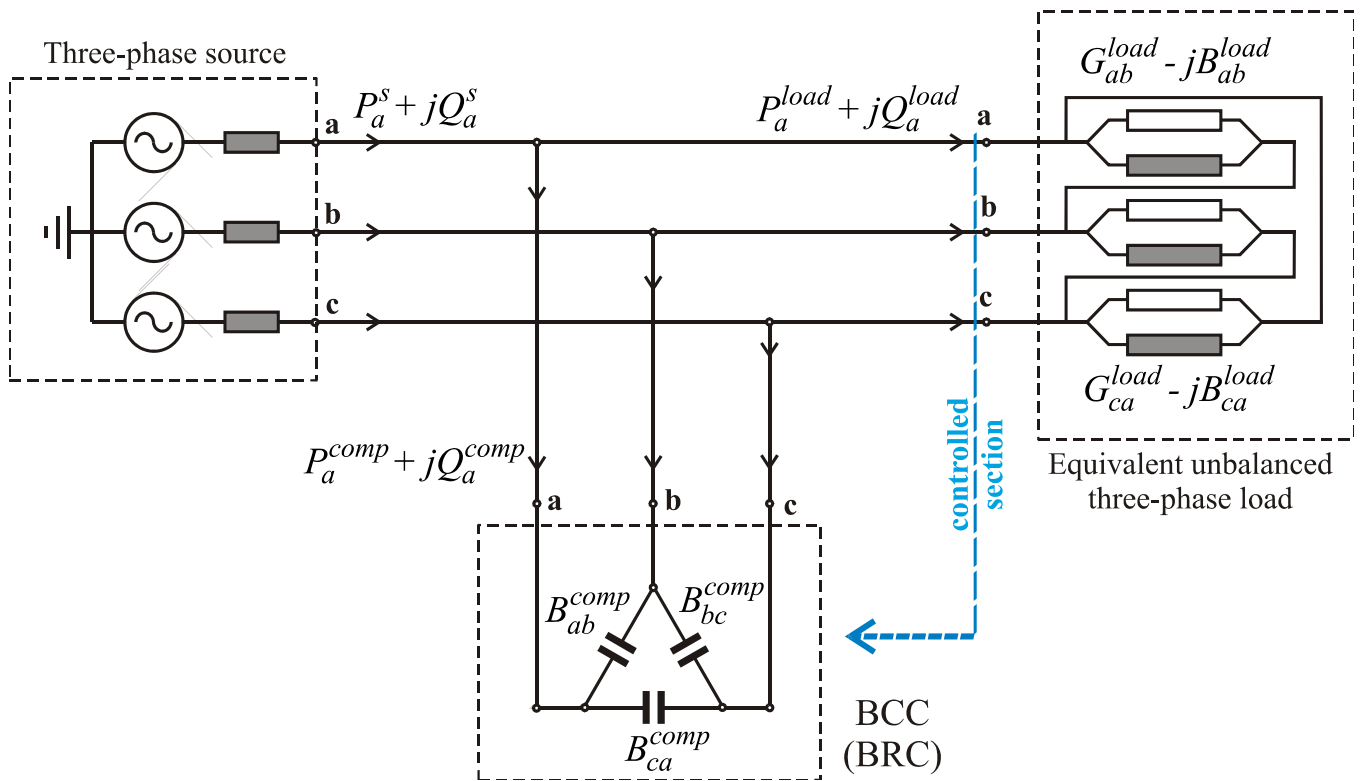
Figure 1. BCC (BRC) for load balancing in a three-phase three-wire network.

As with any delta-connected circuit, the zero-sequence component of the load phase currents is zero:

$$\underline{I}^{load-} \neq 0, \quad \underline{I}^{load0} = 0, \tag{2}$$

Those in (2) are also valid for the currents on the BCC phases, which also is in delta connection:

$$\underline{I}^{comp-} \neq 0, \quad \underline{I}^{comp0} = 0, \tag{3}$$

For the symmetrical components of the phase currents absorbed from the source by the load–BRC assembly, relations (4) are valid:

$$
\begin{aligned}
\underline{I}^{s+} &= \underline{I}^{load+} + \underline{I}^{comp+} \\
\underline{I}^{s-} &= \underline{I}^{load-} + \underline{I}^{comp-} \\
\underline{I}^{s0} &= \underline{I}^{load0} + \underline{I}^{comp0} = 0
\end{aligned}
\tag{4}
$$

The sizing of the three BCC susceptances is performed with the aim of total compensation of the negative sequence currents from the currents on the load phases. In addition, the condition of total compensation of the reactive power absorbed from the source is imposed on the positive sequence ($\cos \varphi^{s+} = 1$). The expressions for calculating the susceptances are determined by solving a system of three independent first-degree Equation (5):

$$
\begin{cases}
Im\left(\underline{I}^{s+}\right) = 0 \\
\mathrm{Re}\left(\underline{I}^{s-}\right) = 0 \\
Im\left(\underline{I}^{s-}\right) = 0
\end{cases}
\tag{5}
$$

It results in several forms of expression of the relations for calculating the values of the three susceptances, depending on the quantities known in the section controlled by the BCC (Figure 1), of which the following are noted here [26]:

- depending on the values of the three equivalent susceptances of the load:

$$\begin{bmatrix} B_{ab}^{comp} \\ B_{bc}^{comp} \\ B_{ca}^{comp} \end{bmatrix} = \begin{bmatrix} -1 & 0 & 0 \\ 0 & -1 & 0 \\ 0 & 0 & -1 \end{bmatrix} \cdot \begin{bmatrix} B_{ab}^{load} \\ B_{bc}^{load} \\ B_{ca}^{load} \end{bmatrix} + \frac{1}{\sqrt{3}} \begin{bmatrix} 0 & 1 & -1 \\ -1 & 0 & 1 \\ 1 & -1 & 0 \end{bmatrix} \begin{bmatrix} G_{ab}^{load} \\ G_{bc}^{load} \\ G_{ca}^{load} \end{bmatrix} \tag{6}$$

- depending on the reactive components of the currents on the load phases:

$$\begin{bmatrix} B_{ab}^{comp} \\ B_{bc}^{comp} \\ B_{ca}^{comp} \end{bmatrix} = \frac{1}{3U} \begin{bmatrix} -1 & -1 & 1 \\ 1 & -1 & -1 \\ -1 & 1 & -1 \end{bmatrix} \begin{bmatrix} I_{ar}^{load} \\ I_{br}^{load} \\ I_{cr}^{load} \end{bmatrix} \tag{7}$$

- depending on the reactive power components in the load phases:

$$\begin{bmatrix} B_{ab}^{comp} \\ B_{bc}^{comp} \\ B_{ca}^{comp} \end{bmatrix} = \frac{1}{3U^2} \cdot \begin{bmatrix} -1 & -1 & 1 \\ 1 & -1 & -1 \\ -1 & 1 & -1 \end{bmatrix} \cdot \begin{bmatrix} Q_a^{load} \\ Q_b^{load} \\ Q_c^{load} \end{bmatrix} \tag{8}$$

- depending on the real and imaginary parts of the sequence components of the load currents:

$$\begin{bmatrix} B_{ab}^{comp} \\ B_{bc}^{comp} \\ B_{ca}^{comp} \end{bmatrix} = \frac{1}{3U} \cdot \begin{bmatrix} 1 & -\sqrt{3} & 1 \\ 1 & 0 & -2 \\ 1 & \sqrt{3} & 1 \end{bmatrix} \cdot \begin{bmatrix} Im\left(\underline{I}^{load+}\right) \\ Re\left(\underline{I}^{load-}\right) \\ Im\left(\underline{I}^{load-}\right) \end{bmatrix} \tag{9}$$

In (6)–(9) with U, the rms value of the phase voltage belonging to the symmetrical three-phase set provided by the source was noted.

The way in which the BCC, containing only reactive circuit elements, achieves the balancing of the active power on the network phases can be deduced from the expressions of the active powers flowing on the BCC phases, written according to the active powers on the load phases:

$$\begin{bmatrix} P_a^{comp} \\ P_b^{comp} \\ P_c^{comp} \end{bmatrix} = \frac{1}{3} \cdot \begin{bmatrix} -2 & 1 & 1 \\ 1 & -2 & 1 \\ 1 & 1 & -2 \end{bmatrix} \cdot \begin{bmatrix} P_a^{load} \\ P_b^{load} \\ P_c^{load} \end{bmatrix} \tag{10}$$

According to [26], if it is noted with P_{av}^{load} the arithmetic mean of the active powers on the load phases,

$$P_{av}^{load} = \frac{1}{3} \left(P_a^{load} + P_b^{load} + P_c^{load} \right) \tag{11}$$

(10) can be written in the form:

$$\begin{aligned} P_a^{comp} &= P_{av}^{load} - P_a^{load} \\ P_b^{comp} &= P_{av}^{load} - P_b^{load} \\ P_c^{comp} &= P_{av}^{load} - P_c^{load} \end{aligned} \tag{12}$$

It is observed that:

$$P_a^{comp} + P_b^{comp} + P_c^{comp} = 0 \tag{13}$$

which means that BCC does not change the active power flow on the whole of the three phases. But on one of the phases (or on two phases) BCC takes active power ($P > 0$) from the network, which it then feeds back into the network on the other two phases (or on the third phase). The value of the active power taken or discharged on each BCC phase is equal to the algebraic difference between the value of the active power of the load on the

respective phase and the average value of the active power on the load phases (12). This is how the active powers are equalized in the phases of the load-BCC assembly:

$$P_a^s = P_a^{load} + P_a^{comp} = P_{av}^{load}$$
$$P_b^s = P_b^{load} + P_b^{comp} = P_{av}^{load}$$
$$P_c^s = P_c^{load} + P_c^{comp} = P_{av}^{load}$$

(14)

Regarding the reactive power flow, on each phase of the BCC results in a reactive power equal and of the opposite sign to that on the homologous phase of the load, so that the load–BCC assembly works at a unit power factor on each phase:

$$Q_a^{comp} = -Q_a^{load}$$
$$Q_b^{comp} = -Q_b^{load}$$
$$Q_c^{comp} = -Q_c^{load}$$

(15)

$$Q_a^s = Q_a + Q_a = 0$$
$$Q_b^s = Q_b + Q_b = 0$$
$$Q_c^s = Q_c + Q_c = 0$$

(16)

The analysis of sequence components (symmetrical) allows us to understand the mechanism of compensation of the unwanted components of the load sequence currents. The relations for the currents on the respective load phases of the BCC, written in terms of the symmetrical components of the load currents, are:

$$\begin{bmatrix} \underline{I}_a^{load} \\ \underline{I}_b^{load} \\ \underline{I}_c^{load} \end{bmatrix} = \begin{bmatrix} 1 \\ a^2 \\ a \end{bmatrix} \cdot \underline{I}^{load+} + \begin{bmatrix} 1 \\ a \\ a^2 \end{bmatrix} \cdot \underline{I}^{load-}$$

(17)

$$\begin{bmatrix} \underline{I}_a^{comp} \\ \underline{I}_b^{comp} \\ \underline{I}_c^{comp} \end{bmatrix} = \begin{bmatrix} 1 \\ a^2 \\ a \end{bmatrix} \cdot \underline{I}^{comp+} + \begin{bmatrix} 1 \\ a \\ a^2 \end{bmatrix} \cdot \underline{I}^{comp-} = -j \begin{bmatrix} 1 \\ a^2 \\ a \end{bmatrix} \cdot Im\left(\underline{I}^{load+}\right) - \begin{bmatrix} 1 \\ a \\ a^2 \end{bmatrix} \cdot \underline{I}^{load-}$$

(18)

So, for the currents on the source phases results:

$$\begin{bmatrix} \underline{I}_a^s \\ \underline{I}_b^s \\ \underline{I}_c^s \end{bmatrix} = \begin{bmatrix} \underline{I}_a^{load} + \underline{I}_a^{comp} \\ \underline{I}_b^{load} + \underline{I}_b^{comp} \\ \underline{I}_c^{load} + \underline{I}_c^{comp} \end{bmatrix} = \begin{bmatrix} 1 \\ a^2 \\ a \end{bmatrix} \cdot Re\left(\underline{I}^{load+}\right)$$

(19)

Therefore, BCC fully compensates for the negative sequence component and the imaginary (reactive) part of the positive sequence component of the load currents. During the phases of the load–BCC assembly, the currents form a set of positive sequences, containing only the real (active) component. The result is therefore the perfect balancing of the active powers and the total elimination of the reactive power taken from the source.

In practice, in a large part of the situations, the active and reactive powers unbalances on the phases of the loads are not excessive, so by applying the (6)–(9) for the equivalent susceptances of the BCC, negative values are obtained. They will therefore have a capacitive character and will be realized practically only by single-phase capacitor banks.

For the three susceptances of the compensator to be negative (or zero), from (8) the condition of simultaneous fulfilment of the following three conditions is deduced:

$$Q_a^{load} + Q_b^{load} \geq Q_c^{load}$$
$$Q_b^{load} + Q_c^{load} \geq Q_a^{load} \qquad (20)$$
$$Q_c^{load} + Q_a^{load} \geq Q_b^{load}$$

If at least one of the (20) is not satisfied, the perfect load balancing, simultaneously with the total compensation of its reactive power by using a BCC, can only be obtained by a capacitive overcompensation. This capacitive overcompensation is sometimes necessary, for example when there is a two-way power transfer through the connection node of the compensator.

When there are no other requirements, capacitive overcompensation, if accepted, should in most cases be minimized. In order not to change the negative sequence component of the currents on the compensator phases, the values obtained with (8) will be corrected with the same, negative value, which means the increase in the compensation capacitive-reactive power on the positive sequence. This value will be proportional to that of the susceptance components involved in the positive sequence current flow:

$$B_{ab}^{comp+} = B_{bc}^{comp+} = B_{ca}^{comp+} = -\frac{Q_t^{load}}{9 \cdot U^2} = -\frac{Q_{av}^{load}}{3 \cdot U^2} \qquad (21)$$

where Q_t^{load} and Q_{av}^{load} are total inductive-reactive power and average reactive power absorbed by the load.

$$Q_t^{load} = Q_a^{load} + Q_b^{load} + Q_c^{load} \qquad (22)$$

$$Q_{av}^{load} = \frac{Q_t^{load}}{3} \qquad (23)$$

If noted with k_Q^+ the proportionality factor applied to supplement the capacitive compensation on the positive sequence, the corrected values of the BCC susceptances will be:

$$\begin{bmatrix} B_{ab}^{comp*} \\ B_{bc}^{comp*} \\ B_{ab}^{comp*} \end{bmatrix} = -\frac{1}{3 \cdot U^2} \left(\begin{bmatrix} 1 & 1 & -1 \\ -1 & 1 & 1 \\ 1 & -1 & 1 \end{bmatrix} \begin{bmatrix} Q_a^{load} \\ Q_b^{load} \\ Q_c^{load} \end{bmatrix} + k_Q^+ \begin{bmatrix} 1 \\ 1 \\ 1 \end{bmatrix} Q_{av}^{load} \right) \qquad (24)$$

When the sum of the reactive powers flowing on the load phases is positive, the minimum value of the capacitive overcompensation that ensures the perfect load balancing by using a BCC, is obtained when:

$$k_Q^+ = \max(M_1, \ M_2, \ M_3) \qquad (25)$$

where:

$$\begin{bmatrix} M_1 \\ M_2 \\ M_3 \end{bmatrix} = \frac{1}{Q_{av}^{load}} \cdot \begin{bmatrix} -1 & -1 & 1 \\ 1 & -1 & -1 \\ -1 & -1 & 1 \end{bmatrix} \cdot \begin{bmatrix} Q_a^{load} \\ Q_b^{load} \\ Q_c^{load} \end{bmatrix} \qquad (26)$$

The relationships presented above are part of a complex mathematical model, presented in detail in [26], except Equations (7), (8) and (10) and, respectively, (20)–(26), obtained by extending the same mathematical model and which were presented for the first time in this article.

Both the relations for sizing the susceptances of the BCC (BRC) composition (6)–(9) and those for explaining the energy mechanism of the load balancing (10)–(19) were based on the conditions related to the three-phase load balancing. Among these relationships, those that use the active and reactive powers on the load phases allow us to obtain an important conclusion: they remain valid regardless of the flowing way of the active and reactive

powers, which can even be simultaneously different on different phases. This conclusion transforms the BCC from a means of load balancing, to one of power flow balancing.

The purpose of this article is to demonstrate the validity of the mathematical model presented above even in the case of two-way active and reactive power flow on the network phases, in the section controlled by the BCC. The best example for such a situation and at the same time the best application for a BCC, more precisely an ABCC with the function of power flow dynamic balancing in a three-phase three-wire network, is that of medium voltage distribution networks with a high concentration of distributed renewable sources of electricity. During periods of time with excess generated power, on different phases, the active and reactive powers can have both different values and different flowing ways. In addition, in the same phase, the way of the active power flow can be different from that of the reactive power (Figure 2).
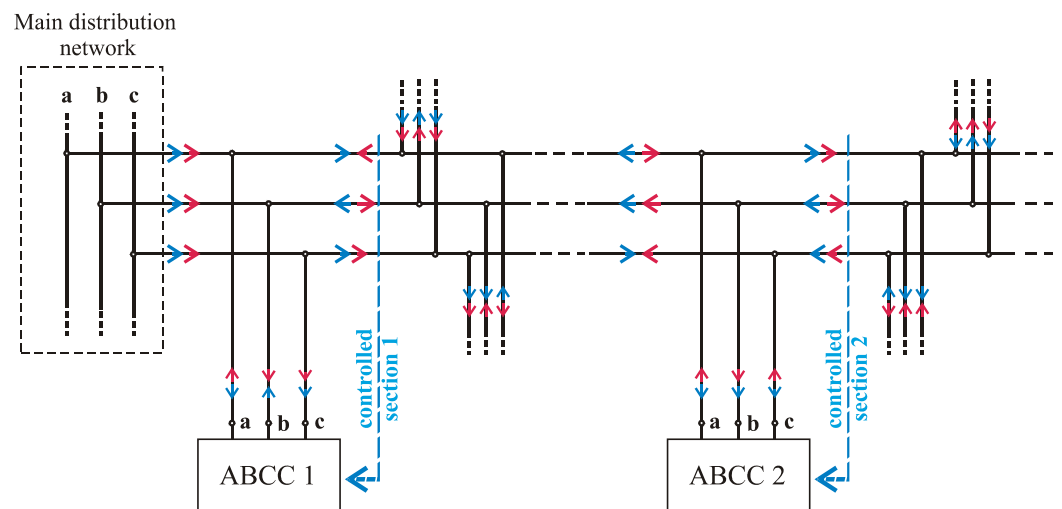

Figure 2. ABCC used for power flow balancing in a three-phase three-wire network.

Capacitive balancing compensators can be used by consumers for load balancing, respectively, by the distribution operator for two-way power flow balancing on network sections (Figure 2). In the case of extended networks with high concentrations of distributed renewable sources, to benefit from the positive effects of power flow balancing on the network sections, this operation must be carried out in several sections of the network, depending on its complexity. The number and capacitive-reactive power installed in the compensators is determined by solving a technical–economic optimization problem.

The expected effects of power flow balancing on the network sections are:

- reducing the asymmetry of the three-phase voltages;
- placing the rms voltage values at the consumer terminals within the admissible limits by reducing the maximum voltage losses on the phases;
- avoiding thermal overloading of the current paths on the network sections;
- reducing the level of unbalance disturbances transferred to the main network.

3. Power Flow Balancing in a Medium Voltage Distribution Network with a High Concentration of DERs (Case Study)

For the study of the ABCC operation, a three-phase distribution network area (Figure 3) was considered, the structure of which was chosen so that the unbalanced power flow on the phases and the propagation of the asymmetry disturbance on the lines and transformers could be highlighted.
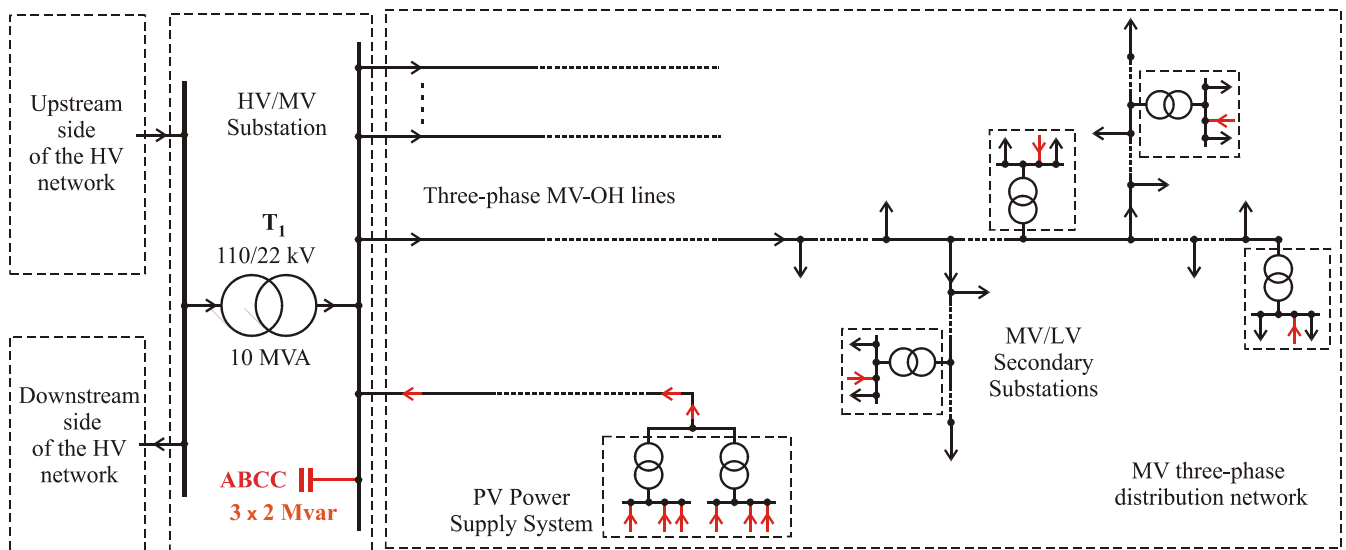
Figure 3. The area of the three-phase distribution network containing a PV Power Supply System.

The source of the unbalance disturbance is the equivalent unbalanced loads, including single-phase prosumers, connected to the LV network. To achieve the two-way transfer of power through the HV/MV substation, a PV Power Supply System was installed in the network. The role of optimizing the operating regime by power flow balancing and improving the power factor falls to the ABCC, which is installed on the medium voltage busbars of the HV/MV substation, i.e., in the vicinity of the common coupling point between the distribution network and the higher voltage network.

The analysis tool used was Matlab-Simulink, due to its ability to model three-phase networks operating under unbalanced regimes. The effects of unbalanced power flow in the MV three-phase distribution network are evaluated on a simplified model, obtained by reducing the real network to an equivalent network (Figure 4), consisting of:

- an equivalent three-phase medium voltage overhead line;
- an equivalent transformer station MV/LV;
- an equivalent three-phase unbalanced load connected to LV.

The PV Power Supply System (PV Power Supply System) is equivalent to a balanced three-phase supplying source connected to LV and an equivalent LV/MV transformer substation. A medium voltage overhead line allows its connection to the network area studied.

To analyze the ABCC efficiency, two relevant operating regimes were considered in which the power flow is unbalanced in the phases:

- Regime 1—winter, morning load peak—the PV system generates a high-value active power, but less than the value of the active power consumed in the RED—the active power flows from the PV system to the MV RED
- Regime 2—summer, daytime no-load—the PV system generates a high-value active power, higher than the value of the active power consumed in the RED—the active power flows from the RED to the HV network.

For both regimes, the equivalent load was modelled in Simulink by impedances of constant values, in the parallel R-L scheme. Considering the values of active and reactive power per phase given in Table 1, symmetrical phase voltage supply of rms values are equal to the rated value, and the values of the equivalent parameters specified in the same table correspond.
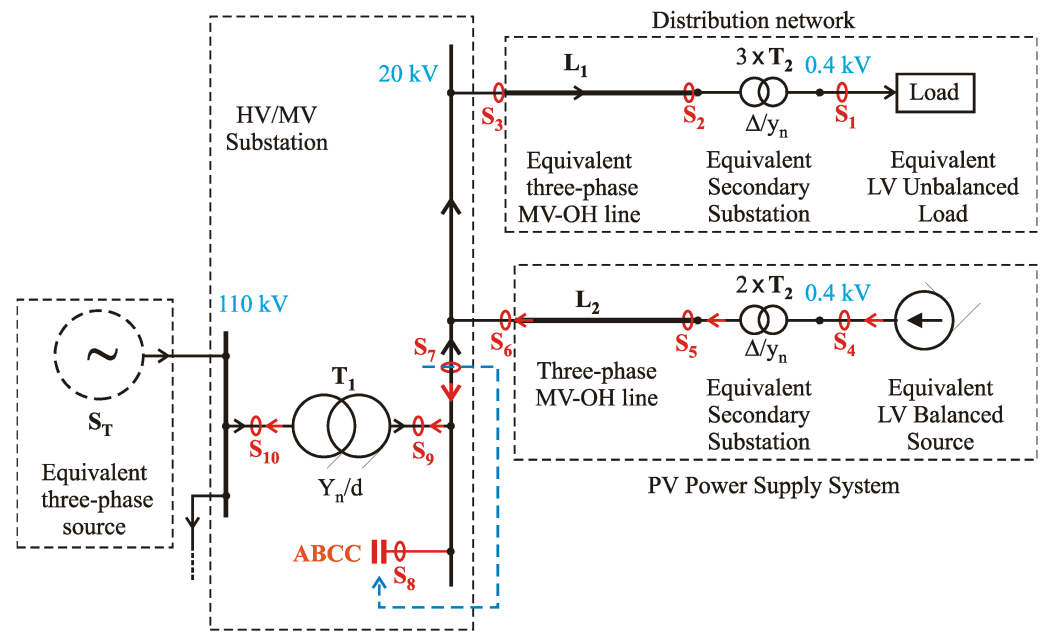
Figure 4. The simplified network consists of equivalent elements.

Table 1. Modelling the equivalent LV unbalanced load (constant shunt impedance, parallel scheme, Yg connection).

Operating Regime	Phase Power Values for Rms Phase Voltage Values $U = U_r/\sqrt{3} = 0.231$ kV	The Values of the Shunt Equivalent Parameters
Regime 1	$P_a^{load} = 2000$ kW, $Q_a^{load} = 700$ kvar $P_b^{load} = 1500$ kW, $Q_b^{load} = 900$ kvar $P_c^{load} = 1700$ kW, $Q_c^{load} = 400$ kvar $P_t^{load} = 5200$ kW, $Q_t^{load} = 2000$ kvar	$R_a = 26.45$ mΩ, $X_{La} = 75.56$ mΩ, $L_a = 0.241$ mH $R_b = 35.27$ mΩ, $X_{Lb} = 58.78$ mΩ, $L_b = 0.187$ mH $R_c = 31.12$ mΩ, $X_{Lc} = 132.25$ mΩ, $L_c = 0.421$ mH
Regime 2	$P_a^{load} = 700$ kW, $Q_a^{load} = 350$ kvar $P_b^{load} = 770$ kW, $Q_b^{load} = 700$ kvar $P_c^{load} = 420$ kW, $Q_c^{load} = 570$ kvar $P_t^{load} = 1890$ kW, $Q_t^{load} = 1620$ kvar	$R_a = 75.57$ mΩ, $X_{La} = 151.14$ mΩ, $L_a = 0.481$ mH $R_b = 68.70$ mΩ, $X_{Lb} = 75.56$ mΩ, $L_b = 0.241$ mH $R_c = 125.95$ mΩ, $X_{Lc} = 92.80$ mΩ, $L_c = 0.295$ mH

The PV source was modelled in both regimes by an assembly of three ideal AC sources, as a result of the fact that the study only considered power flow in the AC network. The equivalent three-phase source was considered to be perfectly phase-balanced, so the three single-phase AC sources draw currents with the same rms value. For the values of the active and reactive powers per phase presented in Table 2, at phase voltages of rms values equal to the rated value, the values of the currents drawn, specified in the same table, resulted.

Table 2. PV Power Supply System modelling (ideal constant current sources, balanced on phases).

Operating Regime	Phase Power Values for Rms Phase Voltage Values $U = U_r/\sqrt{3} = 0.231$ kV	The Values of the Equivalent Current Source's Parameters
Regime 1 and Regime 2	$P_{PVa,b,c} = 1.200$ kW, $Q_{PVa,b,c} = 200$ kvar $\underline{S}_{PVa,b,c} = (1200 + j \cdot 200)$ kVA	$\underline{I}_{PVa} = 5268 \underline{|-\varphi}$ A, $\underline{I}_{PVb} = 5268 \underline{|-(120° - \varphi)}$ A, $\underline{I}_{PVc} = 5268 \underline{|+(120° - \varphi)}$ A, $\varphi = 5°$

The numerical analysis of the power flow in the two regimes, in phase components, is reflected in the form of the values of active powers, reactive powers and phase voltages, and, in sequence components, is reflected in the rms values and phase shift angles of the phase currents and voltages sequence components. For the negative and zero-sequence components, values expressed in relative percent units with respect to the corresponding positive-sequence components were also calculated.

The values of the three-equivalent capacitive susceptances of ABCC were calculated with (8), in which the values of the electrical quantities of section S_7 (the controlled section) were entered. In this section, the distribution network is seen as an unbalanced load (Regime 1) and as an unbalanced source (Regime 2).

For the two regimes studied, the values of the three equivalent capacities of the ABCC were obtained, listed in Table 3.

Table 3. The values of the equivalent capacities of the BCC in the two regimes.

Capacitance	Regime 1	Regime 2
C_{ab}	7.371 μF	0.0728 μF
C_{bc}	8.083 μF	5.3075 μF
C_{ca}	1.465 μF	3.2753 μF

From the numerical analysis carried out by simulating the two regimes, the values that were concentrated in Tables 4 and 5 were extracted. For both cases, the following observations and conclusions are valid:

1. The zero-sequence components of currents and voltages appear only in the areas of three-phase four-wire circuits, more precisely in the secondaries of T2-type transformers, located at the low voltage level (sections S_1 and S_4). This observation is confirmation of the correctness of the modelling, knowing that the delta connection interrupts the propagation of the zero-sequence components of the currents.
2. On the branch S_1–S_2–S_3 the negative sequence components of the currents are propagated, the source of the asymmetry disturbance being the unbalanced load. There is no negative sequence current flow on the branch S_4–S_5–S_6 and therefore the negative sequence components of the voltages are zero, as a result of the fact that the PV source is perfectly balanced. The current unbalance disturbance is also found in section S_7, which is the section considered for the sizing (adjustment) of the capacitance values of the ABCC (controlled section).
3. The power flow in the two regimes is completed in the presence of the ABCC, so that in section S_9 and from the high voltage network S_{10}, the assembly formed by ABCC (S_8)—the distribution network (S_7)—is seen as perfectly balanced, as a three-phase active power load (Regime 1) or as a three-phase active power source (Regime 2).
4. Comparing the values of the active powers and the reactive powers from sections S_7 and S_8, the operation mode of the ABCC is found, also resulting from the mathematical model (10)–(16). Thus, in order to balance the active powers on each phase, ABCC takes over or delivers an active power whose value is equal to the algebraic difference of the active power on the respective phase of the controlled section S_7, and the arithmetic mean of the values of the three active powers on the phases (confirmation of 12). On each phase of section S_9 the values of active powers are equal to the arithmetic mean of the values of active powers in section S_7 (confirmation of 14). For the compensation of the inductive-reactive power on the phases of the controlled section S_7, ABCC absorbs from the network on each phase a capacitive-reactive power of the same value as the inductive-reactive power on the corresponding phase of the load (confirmation of 15). It can be said that the inductive-reactive power on each phase of the load is taken from the BCC so that the higher voltage network discharges the reactive power required to supply the load.

5. On each phase of ABCC (S_8), the value of the reactive power is negative, and it has a capacitive character, which seems natural. ABCC is a reactive power source. But it is not as natural as ABCC, although it is composed only of capacitors, to also intervene in the active power flow in the network. As can be seen from the simulation results, in some phases, it takes active power from the network and in others it feeds back active power to the network. The sum of the values of the active powers taken is equal to the sum of the active values delivered (confirmation of the 13). It can be said that ABCC makes a redistribution of the active power between the phases of the network until they are balanced. On the set of the three phases of the ABCC, the algebraic sum of the active powers is zero (confirmation of the 13).
6. The load balancing effect in the secondary of the T1 transformer in the HV/MV substation is also seen from the sequence current flow. Practically the negative sequence components of the currents in the controlled section S_7 are equal in rms value and are in phase opposition to the negative sequence components of the currents on the ABCC phases (S_8), compensating each other (confirmation of the 17 and 18). In sections S_9 and S_{10} the currents have only positive sequence components (confirmation of the 19).
7. In the presence of ABCC, a perfectly balanced three-phase equivalent load (Regime 1) or a perfectly balanced three-phase active power source (Regime 2) is "seen" in the secondary of the T1 transformer (S_9), so that in all sections on the busbars of MV of the substation and on their derivations (S_3, S_6, S_7, S_8, S_9), the voltages are perfectly symmetrical.

Table 4. The results of the power flow computation—Regime 1.

Electrical Quantity		S_1	S_2	S_3	S_4	S_5	S_6	S_7	S_8	S_9	S_{10}
P_a [kW]		1963.78	1984.71	2091.7	−1248.86	−1235.2	−1203.3	888.4	−234.98	653.41	690.87
P_b [kW]		1492.8	1777.36	1885.04	−1248.88	−1235.2	−1203.3	681.74	−28.32	653.41	690.87
P_c [kW]		1769.88	1525.13	1593.4	−1248.88	−1235.2	−1203.3	390.1	263.31	653.41	690.87
ΣP [kW]		5226.48	5287.2	5570.14	−3746.62	−3705.6	−3609.9	1960.24	≈0	1960.23	2072.61
Q_a [kvar]		687.32	615.18	685.8	−174.57	−105.03	−76.78	609.01	−608.92	0.088	51.63
Q_b [kvar]		895.7	1070.28	1141.8	−174.56	−105.03	−76.78	1065.09	−1065.00	0.088	51.63
Q_c [kvar]		416.43	704.92	734.87	−174.59	−105.03	−76.78	658.08	−657.99	0.087	51.63
ΣQ [kvar]		1999.45	2390.38	2562.47	−523.72	−315.09	−230.34	2332.18	−2331.91	0.2645	154.89
I^+ [A]		8130	170.4	169	5268	99.68	99.71	83.98	64.28	54.03	10.91
I^-	[A]	1138	23.89	23.91	0.006	0	0	23.91	23.91	0	0
	(%)	(13.99)	(14.02)	(14.14)	(≈0)	(0)	(0)	(28.47)	(37.19)	(0)	(0)
I^0	[A]	175.3	0	0	0	0	0	0	0	0	0
	(%)	(2.15)	(0)	(0)	(0)	(0)	(0)	(0)	(0)	(0)	(0)
U_a [V]		227.9	11,349.3	12,093.01	239.37	12,436.87		12,093.01			63,485.38
U_b [V]		229.44	11,273.49	12,093.01	239.37	12,436.87		12,093.01			63,485.38
U_c [V]		234.67	11,463.78	12,093.01	239.37	12,436.87		12,093.01			63,485.38
U^+ [V]		230.7	11,361.92	12,093.01	239.4	12,436.87		12,093.01			63,485.38
U^-	[V]	4.29	110.7	0.013	0	0.014		0.013			0.07
	(%)	(1.86)	(9.74)	(0)	(0)	(≈0)		(≈0)			(0)
U^0	[V]	0.33	0	0	0	0		0			0
	(%)	(0.14)	(0)	(0)	(0)	(0)		(0)			(0)

Balancing by unbalanced shunt capacitive compensation of a real load, or an equivalent load "seen" in the controlled section, has been extensively presented in previous works [26,29–31]. That is why the focal point of this work is given by the simulation of the network-BCC assembly operation in Regime 2, where, in the controlled section, an unbalanced source is "seen". For this regime, presented below are the bus voltage waveforms, respectively, the side current waveforms. The most relevant waveforms are those of the voltage on the MV busbars of the substation, respectively of the currents through the close sections S_3, S_6, S_7, S_8, S_9. They are presented in Figure 5. The scale of currents is graduated in amperes, that of voltage in volts, and of time in seconds.

Table 5. The results of the power flow computation—Regime 2.

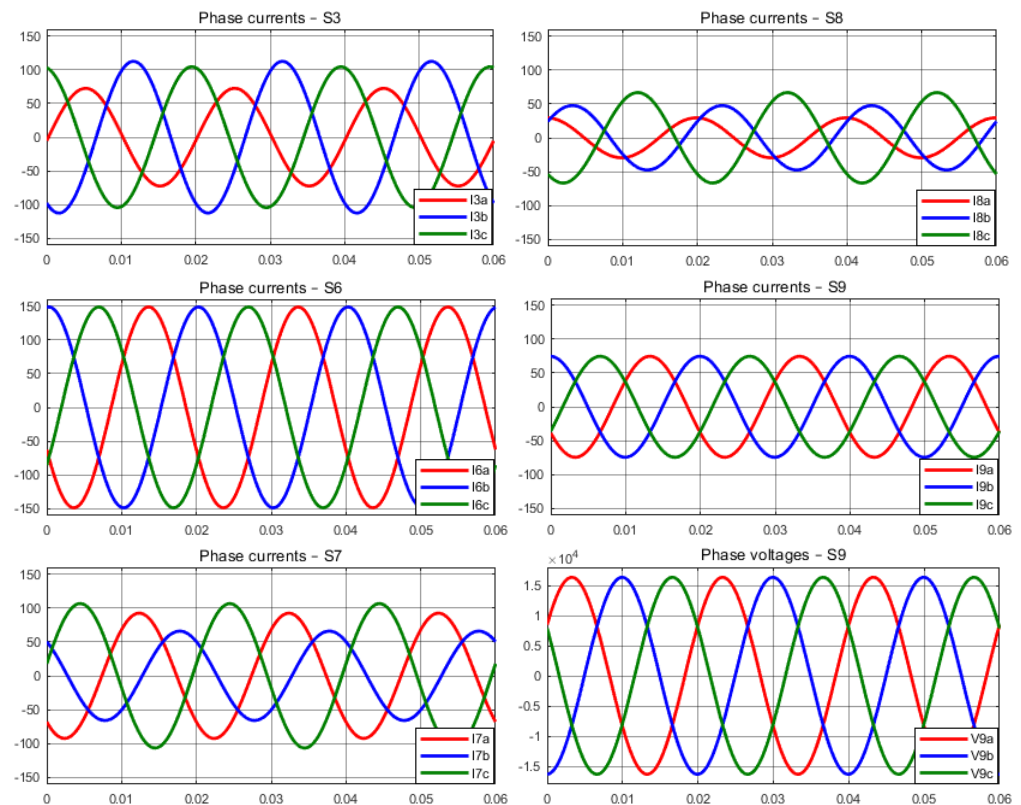| Electrical Quantity		S$_1$	S$_2$	S$_3$	S$_4$	S$_5$	S$_6$	S$_7$	S$_8$	S$_9$	S$_{10}$
P_a [kW]		652.5	472.63	481.36	−1255.24	−1240.98	116.27	−724.24	116.27	−607.97	−570.57
P_b [kW]		688.1	766.88	787.58	−1255.24	−1240.98	−190.05	−418.03	−190.05	−608.08	−570.67
P_c [kW]		388.1	505.73	523.84	−1255.27	−1240.98	73.78	−681.77	73.78	−608.00	−570.68
ΣP [kW]		1728.7	1745.24	1792.78	−3765.75	−3722.96	≈0	−1824.04	≈0	−1824.05	−1711.94
Q_a [kvar]		326.25	372.58	342.97	−240.74	−164.5	−210.54	210.66	−210.54	0.12	48.22
Q_b [kvar]		625.54	487.47	470.72	−240.76	−154.5	−338.34	338.41	−338.34	0.07	48.29
Q_c [kvar]		526.71	691.54	672.03	−240.82	−164.5	−539.73	539.73	−539.73	0.002	48.17
ΣQ [kvar]		1478.5	1551.59	1485.72	−722.32	−493.5	−1088.61	1088.8	−1088.61	0.192	144.68
I^+ [A]		3454	69.38	67.19	5268	104.9	105	61.3	31.41	52.63	9.017
I^-	[A]	828.9	16.57	16.58	0	0	0	16.58	16.59	0.006	0.001
	(%)	(23.99)	(23.88)	(24.67)	(0)	(0)	(0)	(27.04)	(52.81)	(≈0)	(≈0)
I^0	[A]	20.55	0	0	0	0	0	0	0	0	0
	(%)	(0.6)	(0)	(0)	(0)	(0)	(0)	(0)	(0)	(0)	(0)
U_a [V]		222.05	11,313.37	11,551.88	242.62	11,928.58		11,551.88			63,510.11
U_b [V]		217.42	11,191.71	11,551.9	242.63	11,928.61		11,551.9			63,510.1
U_c [V]		211.09	11,206.5	11,551.93	242.63	11,928.63		11,551.93			63,510.13
U^+ [V]		220.2	11,237.06	11,551.9	242.6	11,928.61		11,551.9			63,510.1
U^-	[V]	2.83	76.78	0.03	0	0		0.03			0.01
	(%)	(1.28)	(0.68)	(≈0)	(0)	(0)		(≈0)			(≈0)
U^0	[V]	0.035	0	0	0	0		0			0
	(%)	(≈0)	(0)	(0)	(0)	(0)		(0)			(0)

Figure 5. Regime 2—the voltage waveforms on the MV busbars of the substation, respectively, and the waveforms of the currents through the neighbouring sections.

Among the quantitative and qualitative observations resulting from the numerical calculation of the power flow, a part is confirmed by this graphic representation. As can be seen, a time interval of 60 ms was considered, corresponding to the duration of three consecutive cycles. The current waveforms in section S$_7$ are the result of combining the current waveforms in sections S$_3$ and S$_6$. The unbalance disturbance, whose source is the unbalanced equivalent load in section S$_1$, propagates through S$_2$, S$_3$ and then into S$_7$. It is cancelled by ABCC intervention (S$_8$). The current waveforms in section S$_9$, which are the result of combining the current waveforms in sections S$_7$ and S$_8$, show perfect

balancing. A comparison of the currents and voltages in S_9 shows the 10 ms gap (π rad phase shift) between the phase voltage and the current on the same phase, which means that it is a reverse transfer of active powers from the secondary of the transformer from the substation (S_9) to its primary (S_{10}—the higher voltage network), at a unitary power factor. The medium voltage network is therefore seen from the high voltage network as an equivalent balanced source of active power. As a result of the intervention of ABCC, the balancing of the power flow is achieved on the phases, which determines the voltage symmetrization on the medium voltage busbars. The voltage asymmetry disturbance does not propagate to the higher voltage network.

4. Conclusions

The article demonstrates, using a case study carried out by Matlab-Simulink simulation, that a BCC, known for its voltage regulation, power factor improvement and load balancing functions in three-phase networks, can work just as well when the active powers are bidirectional through the controlled section, on one or more phases. The mathematical model, which establishes the relations for calculating the BCC susceptances and demonstrates the balancing mechanism as an effect of the power redistribution between the network phases, remains valid. Of the two regimes presented in the case study, Regime 2 was chosen so that the three-phase medium-voltage network containing DERs injects unbalanced active powers into the higher voltage network, because of the excess active power generated. The effect of the BCC intervention, or more precisely, of its dynamic variant ABCC, consists of maximizing the power factor value simultaneously with the power flow balancing through the substation. This results in voltage symmetrization both on the MV busbars and in the buses of an extended area of the network connected to them. It can be said that ABCC prevents the propagation of unbalance disturbance in the HV network, with the assembly formed by ABCC and the MV network being "seen" from the higher voltage network as a balanced three-phase source of active power.

The article makes an additional argument in favour of the widespread use of ABCCs by extending the load-balancing function and transforming it into a power flow-balancing function. Although it does not have as high a level of technical performance (reaction speed, adjustment precision) as equipment with similar SPC-type functions, the ABCC is preferred for its constructive simplicity, and lower acquisition and operating costs. An ABCC can be installed practically anywhere in the network and can be sized with no maximum limit imposed on the rated capacitive-reactive power. Theoretically, any type of unbalance, however large, can be compensated by an ABCC. However, there is a limitation related to the fact that ABCC injects reactive power into the network. In order not to produce capacitive overcompensation, this reactive power must be taken up by the load. Therefore, the level of unbalance that can be compensated for with an ABCC is higher the lower the value of the power factor is in the controlled section. This condition is compatible with the need to reduce, as much as possible, the value of the inductive-reactive power injected into the network by the DERs inverters, which favours generation efficiency. Thus, ABCCs can be considered sources of inductive-reactive power to cover the needs of the loads, being able to be installed in one or more sections of the network.

Data Availability Statement: Dataset available on request from the authors.

Conflicts of Interest: The authors declare no conflicts of interest.

Abbreviations

DER	Distributed Energy Resources
EPDS	Electric Power Distribution Systems
EV	Electric Vehicles
PCC	Point of Common Coupling
HV/MV/LV	High/Medium/Low Voltage
SPC	Switching Power Converter
LVR	Line Voltage Regulator
OLTC	On-Load Tap Changer
RPC	Reactive Power Compensator
ZSCC	Zero Sequence Current Compensator
D-STATCOM	Distribution Static Synchronous Compensator
DVR	Dynamic Voltage Restorer
UPQC	Unified Power Quality Conditioner
BESS	Battery Energy Storage System
PV	Photo Voltaic
BRC	Balancing Reactive Compensator
ABC	Adaptive Balancing Compensator
SVC	Static var Compensator
CPC	Current's Physical Components
BCC	Balancing Capacitive Compensator
ABCC	Adaptive Balancing Capacitive Compensator

Notations

U, a	phase to ground rms voltage, Stokvis' rotation operator
$\underline{Y}_{ab}^{load}$, $\underline{Y}_{bc}^{load}$, $\underline{Y}_{ca}^{load}$	equivalent admittances of the load in the delta equivalent scheme
G_{ab}^{load}, G_{bc}^{load}, G_{ca}^{load}	equivalent conductances of the load in the delta equivalent scheme
B_{ab}^{load}, B_{bc}^{load}, B_{ca}^{load}	equivalent susceptances of the load in the delta equivalent scheme
$\underline{I}^{load+}$, $\underline{I}^{load-}$, $\underline{I}^{load0}$	phasors of positive, negative and zero sequence components of the phase currents at the three-phase unbalanced load
$\underline{I}^{comp+}$, $\underline{I}^{comp-}$, $\underline{I}^{comp0}$	phasors of positive, negative and zero sequence components of the phase currents at BCC
$\underline{I}^{s+}$, $\underline{I}^{s-}$, $\underline{I}^{s0}$	phasors of positive, negative and zero sequence components of the phase currents at three-phase source
$\cos \varphi^{s+}$	power factor on the positive sequence
B_{ab}^{comp}, B_{bc}^{comp}, B_{ca}^{comp}	the equivalent susceptances on the sides of the delta scheme of the compensator
I_{ar}^{load}, I_{br}^{load}, I_{cr}^{load}	the reactive components of the currents on the load phases;
Q_a^{load}, Q_b^{load}, Q_c^{load}	reactive powers on the load phases
P_a^{load}, P_b^{load}, P_c^{load}	active powers on the load phases
P_a^{comp}, P_b^{comp}, P_c^{comp}	active powers on the BCC phases
P_{av}^{load}	the arithmetic mean value of the active powers on the load phases
P_a^s, P_b^s, P_c^s	active powers on the source phases
Q_a^{load}, Q_b^{load}, Q_c^{load}	reactive powers on the load phases
Q_t^{load}, Q_{av}^{load}	total, respectively average reactive powers of the load
Q_a^{comp}, Q_b^{comp}, Q_c^{comp}	reactive powers on the BCC phases
Q_a^s, Q_b^s, Q_c^s	reactive powers on the source phases
$\underline{I}_a^{load}$, $\underline{I}_b^{load}$, $\underline{I}_c^{load}$	phasors of the phase currents at the three-phase unbalanced load
$\underline{I}_a^{comp}$, $\underline{I}_b^{comp}$, $\underline{I}_c^{comp}$	phasors of the phase currents at BCC
$\underline{I}_a^s$, $\underline{I}_b^s$, $\underline{I}_c^s$	phasors of the phase currents at three-phase source
k_Q^+	proportionality factor applied to supplement the capacitive compensation on the positive sequence

References

1. Khadem, S.K.; Basu, M.; Conlon, M.F. Power quality in grid connected renewable energy systems: Role of custom power devices. In Proceedings of the Conference on Renewable Energies and Power Quality (ICREPQ'10), Granada, Spain, 23–25 March 2010.
2. Pudjianto, D.; Strbac, G.; Boyer, D. Virtual power plant: Managing synergies and conflicts between transmission system operator and distribution system operator control objectives. *CIRED Open Access Proc. J.* **2017**, *2017*, 2049–2052. [CrossRef]
3. Soltani, S.H.; Rashidinejad, M.; Abdollahi, A. Dynamic phase balancing in the smart distribution networks. *Int. J. Electr. Power Energy Syst.* **2017**, *93*, 374–383. [CrossRef]
4. Pratama, N.A.; Rahmawati, Y. Evaluation of unbalanced load impacts on distribution transformer performances. *Front. Energy Syst. Power Eng.* **2020**, *2*, 28–35.
5. Njafi, A.; Iskender, I.; Genc, N. Evaluating and derating of three-phase distribution transformer under unbalanced voltage and unbalance load using finite element method. In Proceedings of the 2014 IEEE 8th International Power Engineering and Optimization Conference (PEOCO2014), Langkawi, Malaysia, 24–25 March 2014.
6. Kersting, W.H. Causes and effects of unbalanced voltages serving an induction motor. *IEEE Trans. Ind. Appl.* **2001**, *37*, 165–170. [CrossRef]
7. Bossio, G.R.; De Angelo, C.H.; Donolo, P.D.; Castellino, A.M.; Garcia, G.O. Effects of voltage unbalance on IM power, torque and vibrations. In Proceedings of the 2009 IEEE International Symposium on Diagnostics for Electric Machines, Power Electronics and Drives, Cargese, France, 31 August–3 September 2009.
8. Kongtrakul, N.; Wangdee, W.; Chantaraskul, S. Comprehensive review and a novel technique on voltage unbalance compensation. *IET Smart Grid* **2023**, *6*, 331–358. [CrossRef]
9. Jahn, R.; Holt, M.; Rehtanz, C. Mitigation of voltage unbalances using a line voltage regulator. In Proceedings of the 2021 IEEE Madrid Power-Tech, Madrid, Spain, 28 June–2 July 2021.
10. Zecchino, A.; Hu, J.; Coppo, M.; Marinelli, M. Experimental testing and model validation of a decoupled-phase on-load tap-changer transformer in an active network. *IET Gener. Transm. Distrib.* **2016**, *10*, 3834–3843. [CrossRef]
11. Czarnecki, L.S.; Haley, P.M. Unbalanced power in four-wire systems and its reactive compensation. *IEEE Trans. Power Deliv.* **2015**, *30*, 53–63. [CrossRef]
12. Montoya-Mira, R.; Blasco, P.A.; Diez, J.M.; Montoya, R.; Reig, M.J. Unbalanced and Reactive Currents Compensation in Three-Phase Four-Wire Sinusoidal Power Systems. *Appl. Sci.* **2020**, *10*, 1764. [CrossRef]
13. Chang, W.N.; Yeh, K.D. Real-time load balancing and power factor correction of three-phase, four-wire unbalanced systems with DSTATCOM. *J. Mar. Sci. Technol.* **2014**, *22*, 8.
14. Subramani, M.B.; Gulipalli, S.C.; Chu, C.C. An improved compensation technique using DVR for power quality improvement in distribution power system. In Proceedings of the 2021 IEEE 2nd International Conference on Smart Technologies for Power, Energy and Control (STPEC), Bilaspur, India, 19–22 December 2021.
15. Abdoli, O.; Gholipour, E.; Hooshmand, R.A. A new approach to compensating voltage unbalance by UPQC-based PAC. *Elec. Power Compon. Syst.* **2018**, *46*, 1769–1781. [CrossRef]
16. Coppo, M.; Raciti, A.; Caldon, R.; Turri, R. Exploiting inverter-interfaced DG for voltage unbalance mitigation and ancillary services in distribution systems. In Proceedings of the 2015 IEEE 1st International Forum on Research and Technologies for Society and Industry Leveraging a better tomorrow (RTSI), Turin, Italy, 16–18 September 2015.
17. Nejabatkhah, F.; Li, Y.W. Flexible unbalanced compensation of three phase distribution system using single-phase distributed generation inverters. *IEEE Trans. Smart Grid* **2019**, *10*, 1845–1857. [CrossRef]
18. Weckx, S.; Driesen, J. Load balancing with EV chargers and PV inverters in unbalanced distribution grids. *IEEE Trans. Sustain. Energy* **2015**, *6*, 635–643. [CrossRef]
19. Islam, M.R.; Lu, H.; Hossain, M.J.; Li, L. Mitigating unbalance using distributed network reconfiguration techniques in distributed power generation grids with services for electric vehicles: A review. *J. Clean. Prod.* **2019**, *239*, 117932. [CrossRef]
20. Shahania, F.; Wolfs, P.J.; Ghosh, A. Voltage unbalance reduction in low voltage feeders by dynamic switching of residential customers among three phases. *IEEE Trans. Smart Grid* **2014**, *5*, 1318–1327. [CrossRef]
21. Islam, M.R.; Lu, H.; Hossain, M.J.; Li, L. Optimal coordination of electric vehicles and distributed generators for voltage unbalance and neutral current compensation. *IEEE Trans. Ind. Appl.* **2021**, *57*, 1069–1080. [CrossRef]
22. Siti, M.W.; Nicolae, D.V.; Jimoh, A.A.; Ukil, A. Reconfiguration and load balancing in the LV and MV distribution networks for optimal performance. *IEEE Trans. Power Deliv.* **2007**, *22*, 2534–2540. [CrossRef]
23. Gyugyi, L.; Otto, R.; Putman, T. Principles and applications of static thyristor-controlled shunt compensators. *IEEE Trans. Power Appl. Syst.* **1978**, *PAS-97*, 1935–1945.
24. Gueth, G.; Enstedt, P.; Rey, A.; Menzies, R.W. Individual phase control of a static compensator for load compensation and voltage balancing. *IEEE Power Eng. Rev.* **1987**, *2*, 898–905.
25. Czarnecki, L.S.; Hsu, S.M.; Chen, G. Adaptive balancing compensator. *IEEE Trans. Power Deliv.* **1995**, *10*, 1663–1669. [CrossRef]
26. Pană, A. Active load balancing in a three-phase network by reactive power compensation. In *Power Quality—Monitoring, Analysis and Enhancement*; Zobaa, A., Ed.; InTech: Rijeka, Croatia, 2011; pp. 219–254.
27. Chang, W.N.; Liao, C.H. Design and implementation of a STATCOM based on a multilevel FHB converter with delta-connected configuration for unbalanced load compensation. *Energies* **2017**, *10*, 921. [CrossRef]

28. Barrios-Martínez, E.; Ángeles-Camacho, C. Technical comparison of FACTS controllers in parallel connection. *J. Appl. Res. Technol.* **2017**, *15*, 36–44. [CrossRef]

29. Pană, A.; Băloi, A.; Molnar-Matei, F. Load balancing by unbalanced capacitive shunt compensation—A numerical approach. In Proceedings of the 2010 14th International Conference on Harmonics and Quality of Power (ICHQP 2010), Bergamo, Italy, 26–29 September 2010.

30. Pană, A.; Băloi, A.; Molnar-Matei, F. From the balancing reactive compensator to the balancing capacitive compensator. *Energies* **2018**, *11*, 1979. [CrossRef]

31. Pană, A.; Băloi, A.; Molnar-Matei, F. New method for calculating the susceptances of a balancing capacitive compensator for a three-phase four-wire distribution network. *Int. J. Electr. Power Energy Syst.* **2020**, *115*, 105414. [CrossRef]